NANO REVIEWS

COACTION PUBLISHING

Short Communication

Stability and aromaticity of $nH_2@B_{12}N_{12}$ ($n = 1$–12) clusters

Santanab Giri, Arindam Chakraborty and Pratim K. Chattaraj*

Department of Chemistry and Center for Theoretical Studies, Indian Institute of Technology Kharagpur, Kharagpur, India

Received: 1 November 2010; Revised: 24 March 2011; Accepted: 25 March 2011; Published: 26 April 2011

Abstract

Standard *ab initio* and density functional calculations are carried out to determine the structure, stability, and reactivity of $B_{12}N_{12}$ clusters with hydrogen doping. To lend additional support, conceptual DFT-based reactivity descriptors and the associated electronic structure principles are also used. Related cage aromaticity of this $B_{12}N_{12}$ and $nH_2@B_{12}N_{12}$ are analyzed through the nucleus independent chemical shift values.

Keywords: *hydrogen storage*; *metal cluster*; *conceptual DFT*; *aromaticity*

Hydrogen as a unique medium for storage and transportation of energy has already become an area worthy of fundamental research. An incessant upsurge in the world population in the last few decades has made a great impact on the different global biomes. A splendid growth in world economy followed by a revolution in architectural ecstasy has undeniably elated the human race, but, regrettably at the cost of ruthless deforestation and consequential global warming that had a heavy toll on our surrounding eco-system. An incessant deforestation with vigorous loss of greenery accompanied by an excessive usage of the fossil fuels has resulted in an environmental imbalance as well as a probable energy crisis that may badly affect us in the future. The possible measures to combat this grave energy shortage have been motivating the scientific minds to propose alternative measures. In this perspective the use of hydrogen as an energy source is equally appealing and demanding. Hydrogen as a fuel is quite advantageous in the sense that it can be easily produced from some common renewable energy sources like hydroelectric, solar, wind, or geothermal with water as the raw material. For releasing the energy, hydrogen may be burnt off to produce water as a harmless byproduct. So hydrogen, unlike the fuel sources, may be conceived as a cleaner and environment-friendly energy reserve (1, 2) and may be used rigorously before the oil reserves are totally depleted. But the lack of appropriate materials for the physical storage of hydrogen in large gravimetric and volumetric densities is the major reason behind its very limited usage in practice. However, several materials like AlN nanostructures (3), transition-metal doped BN systems (4), alkali-metal doped benzenoid (5), and fullerene clusters (6), bare as well as light metal and transition-metal coated boron buckyballs, B_{80} (7), and magnesium clusters (8) have been exercised experimentally and theoretically as capable storage material for hydrogen. Again, owing to the considerable ability of MgH_2 as a hydrogen-storage material, Mg-clusters doped with H_2 molecule have been theoretically investigated and found to be weakly stable or metastable depending on the cluster size (9). Giri et al. (10) have recently demonstrated that small to medium metal clusters involving the trigonal, cationic Li_3^+ and Na_3^+ rings, and the neutral Mg_n and Ca_n [$n = 8$–10] cages, analogous to the metastable hydrogen-stacked Mg_n clusters (9) can be executed for trapping hydrogen effectively in both atomic and molecular forms.

The endohedral (11, 12) as well as exohedral (13) trapping of hydrogen within a BN buckyball reveals that hydrogen dominantly retains its molecular nature in the former case while for the latter mode, the hydrogens are linked in their atomic form with each of the B and N centers. In this article we have made a conceptual density functional theory (DFT) (14–16) based treatment toward conceiving the potential use of a $B_{12}N_{12}$ cage-cluster as an effective storage material for trapping hydrogen in its molecular form. Conceptual DFT (14–16) in conjunction

with its various global reactivity descriptors like electronegativity (17, 18) (χ), hardness (19, 20) (η), and electrophilicity (21, 22) (ω) along with the associated electronic structure principles have been quite effective in providing a meaningful rationale toward describing the stability and associated structural changes of the cage-like $B_{12}N_{12}$ cluster upon gradual binding with molecular hydrogen. An assessment of the stability of the H_2-bound $B_{12}N_{12}$ cage cluster in terms of an aromaticity criterion offers important insights into the possible use of the $B_{12}N_{12}$ cage as an effective hydrogen storage material. The cage aromaticity of the bare as well as hydrogen bound $B_{12}N_{12}$ cluster has been evaluated from the nucleus independent chemical shift (23) (NICS) values at the cage-center computed by exploiting the procedure of Schleyer et al. (23).

1. Theoretical background

The stable state of a molecular species as well as its reactivity during chemical response can be well understood from a careful scrutiny of the behavior of some conceptual density functional theory (CDFT) based global reactivity descriptors like electronegativity (17, 18) (χ), hardness (19, 20) (η), and electrophilicity (21, 22) (ω). Chemical hardness (19, 20) (η) and electrophilicity (21, 22) (ω) do provide useful information that correlates the thermodynamic stability and reactivity of molecular systems. The overall molecular behavior during chemical reactions finds further justification from a scrutiny of the well-established electronic structure principles like the Principles of Maximum Hardness (24, 25) (PMH), Minimum Polarizability (26) (PMP), and Minimum Electrophilicity (27) (PME). The conceptual DFT-based global reactivity descriptors in association with the important electronic structure principles mentioned above seem to be quite significant in analyzing the increasing stability of the $B_{12}N_{12}$ cage with gradual doping of molecular hydrogen. In an N-electron system, the electronegativity (χ) and hardness (η) can be defined as follows:

$$\chi = -\left(\frac{\partial E}{\partial N}\right)_{v(\mathbf{r})} = -\mu, \tag{1}$$

$$\eta = \left(\frac{\partial^2 E}{\partial N^2}\right)_{v(\mathbf{r})}, \tag{2}$$

$$\text{and } \omega = \left(\frac{\chi^2}{2\eta}\right) = \left(\frac{\mu^2}{2\eta}\right), \tag{3}$$

with $v(\mathbf{r})$ and μ as the external and chemical potentials, respectively.

Using finite difference method, electronegativity, and hardness can be expressed as follows:

$$\chi = \frac{(IP + EA)}{2} \text{ and } \eta = (IP - EA), \tag{4}$$

where IP and EA are the ionization potential and electron affinity, respectively.

If E_{HOMO} and E_{LUMO} are the energies of the highest occupied and the lowest unoccupied molecular orbitals then Equation 4 can be written as:

$$\chi = -\frac{(E_{HOMO} + E_{LUMO})}{2} \text{ and}$$
$$\eta = (E_{LUMO} - E_{HOMO}). \tag{5}$$

2. Computational details

The optimization of the molecular geometries of the different $nH_2@B_{12}N_{12}$ ($n = 1$–12) systems are carried out at the B3LYP/6-311+G(d) level of theory using the GAUSSIAN 03 program (28) suite. The convergence criterion for all the cage-complexes is fulfilled with the attainment of a stationary point. This implies that the optimized cage-complexes do exist at minima positions on the potential energy surface (PES). Single-point calculations of these structures, optimized at the B3LYP level, are further done at the MP2 level of theory using the same basis set. The energies of the highest occupied molecular orbital (HOMO) and the lowest unoccupied molecular orbital (LUMO) for all the clusters are computed from the corresponding MP2 single-point calculations. The ionization potential (IP) and electron affinity (EA) of the H_2-trapped clusters are evaluated using Koopmans' approximation (29). Different conceptual DFT-based reactivity descriptors are calculated using the standard protocol. The cage aromaticity of the various $nH_2@B_{12}N_{12}$ ($n = 1$–12) clusters are assessed from the corresponding nucleus independent chemical shift (NICS) values computed using Schleyer's technique (23). To explain the stability of the doped clusters and spontaneity of these H_2 trapping reactions on $B_{12}N_{12}$ we calculate the following energy parameters:

$$\text{Interaction energy (IE)} = E_{nH_2(BN)_{12}} - [E_{(BN)_2} + nH_2];$$
$$n = \text{no. of molecular } H_2, \tag{6}$$

$$\text{Gain in energy } (GE) = E_{(n-1)H_2(BN)_{12}} + E_{H_2} - E_{nH_2(BN)_{12}}, \tag{7}$$

and

$$\text{Chemisorption energy } (CE) = \frac{2}{n}\left[E_{(BN)_{12}} + \frac{n}{2}E_{H_2} - E_{(BN)_{12}H_n}\right];$$
$$n = \text{no. of H atoms.} \tag{8}$$

3. Results and discussion

Total energy (E_{Tot}, au) and conceptual DFT-based global reactivity descriptors like electronegativity (χ, eV), hardness (η, eV), and electrophilicity (ω, eV) of the bare as well as several H_2-bound $B_{12}N_{12}$ cage-complexes are

Citation: Nano Reviews 2011, 2: 5767 - DOI: 10.3402/nano.v2i0.5767

presented in Table S1 (Appendix). The reaction electrophilicity ($\Delta\omega$), interaction energy per hydrogen molecule ($E_{IE/H2}$), gain in energy (E_{GE}), and the dissociative chemisorption energy (E_{CE}) values computed for some plausible reactions depicting the gradual trapping (calculations are performed by increasing the number of H_2 molecules being trapped) of H_2 onto the $B_{12}N_{12}$ cage are provided in Table S2 (Appendix). Different energy components suggest that the H_2-encapsulated clusters are stable but not very stable so that both adsorption and desorption become favorable as is required for $B_{12}N_{12}$ to be a good storage material. The adsorption is somewhere in between physisorption and chemisorption. The optimized molecular geometries of the $B_{12}N_{12}$ cage and some of its dominant H_2-bound analogous are depicted in Fig. 1. A cumulative plot of the variation of the allied global descriptors and the associated energy parameters as a function of cluster growth (upon gradual H_2-binding) for the corresponding nH_2-trapped $B_{12}N_{12}$ complexes are shown in Fig. 2. Fig. 3 describes the variation of the aromaticity criterion of the bare and nH_2 bound $B_{12}N_{12}$ clusters computed in terms of their NICS(0) values. An intrinsic reaction coordinate (IRC) profile for a model reaction describing the binding of a single H_2 molecule with a BN moiety is depicted in Fig. 4. Analyzing the relative activation barriers, it may be assumed that the adsorption is faster than the desorption but the rate of the latter is not very low as required. The important frontier molecular orbitals (HOMO and LUMO) of $B_{12}N_{12}$ clusters and some of its representative $nH_2@B_{12}N_{12}$ cage-complexes are portrayed in Fig. 5. A careful scrutiny of Table S1 reveals that the electronegativity of the different nH_2 bound $B_{12}N_{12}$ clusters shows on an average a falling trend that further presumes a reluctance of the above cluster assemblies toward accepting further electrons. This opinion regarding an increment in the molecular stability with gradual cluster growth (upon H_2-binding) is well substantiated from the respective trends of the hardness (η) and electrophilicity (ω) values vis-à-vis the PMH and the PME. While the chemical hardnesses of the various nH_2-trapped $B_{12}N_{12}$ analogues show mostly an increasing trend with an increase in the cluster size, the electrophilicities of the respective cluster moieties reveal an equivalent mode of decline in most cases. Table S2 makes an attempt in analyzing the tendency of the $B_{12}N_{12}$ cage toward gradual hydrogen storage through a moderate correlation between the reaction electrophilicity ($\Delta\omega$) and other associated energy parameters for a set of plausible H_2-trapping reactions. The reaction electrophilicity ($\Delta\omega$) and interaction energy per hydrogen molecule ($E_{IE/H2}$) for all the trapping reactions are negative and in that way proving their stability toward the resultant nH_2-bound $B_{12}N_{12}$ cage-complexes as dictated by the PME. An analysis of the related free energy changes might have been more useful in this case. The gain in energy (E_{GE}) and the dissociative chemisorption energies (E_{CE}) of the aforesaid reactions are on the other hand positive as anticipated. The E_{GE} values exhibit an unusual trend but nonetheless increases with gradual hydrogen storage

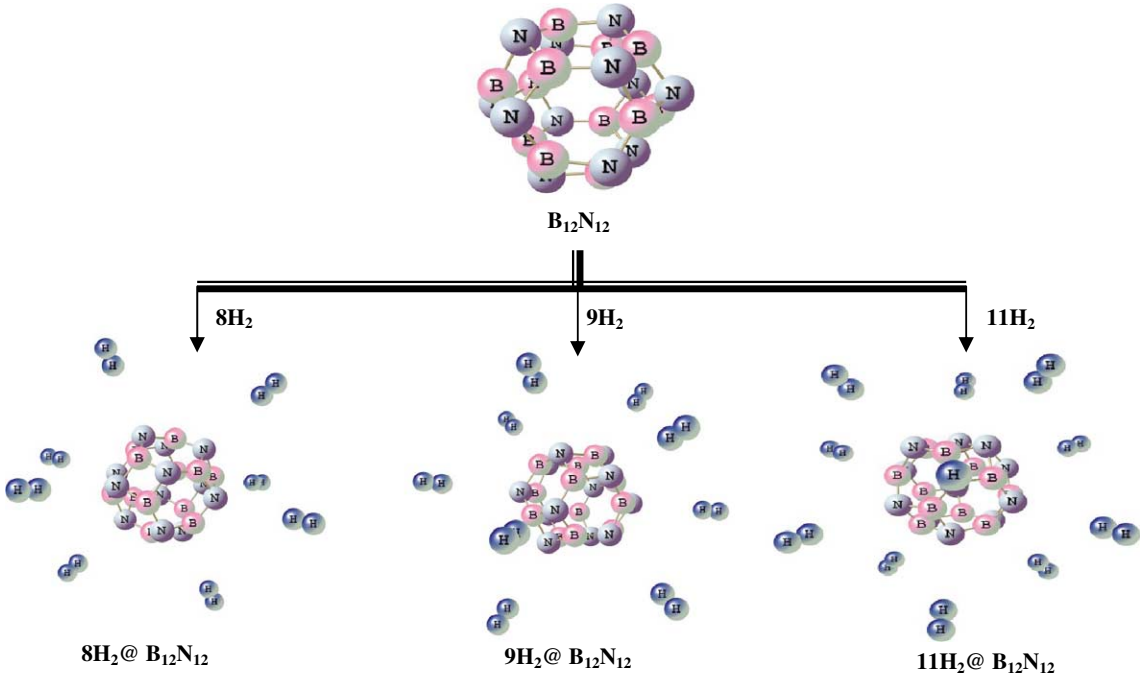

Fig. 1. Optimized geometries (B3LYP/6-311+G(d)) of $B_{12}N_{12}$ and some representative $nH_2@B_{12}N_{12}$ structures.

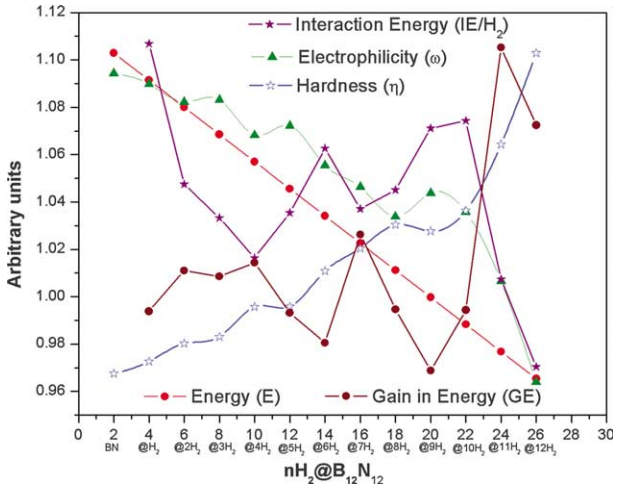

Fig. 2. Plots of all the quantities in Table S1 for different $nH_2@B_{12}N_{12}$ systems.

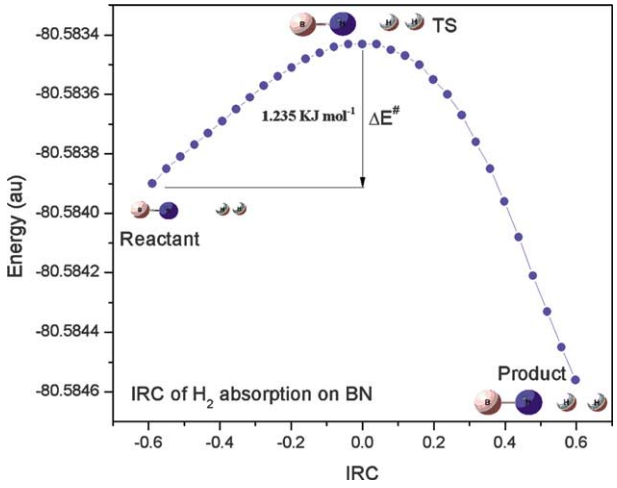

Fig. 4. Energy profile for H_2 absorption on single BN molecule along the intrinsic reaction coordinate.

thereby establishing the stability of the nH_2-trapped $B_{12}N_{12}$ clusters in comparison to the bare $(BN)_{12}$ analogues. The variation of the various global reactivity descriptors and the associated energy parameters depicted pictorially in Fig. 2 explicitly clarifies the molecular stability and non-spontaneity toward chemical reactivity of the nH_2-trapped $B_{12}N_{12}$ clusters from the perspective of conceptual DFT and reaction energetics, respectively. The molecular hardness (η) of the $B_{12}N_{12}$ cage shows a more or less steady increase upon hydrogen loading onto the same. Such an increment in the η profile is anticipated by an analogous decreasing trend of the corresponding global electrophilicity (ω). An analysis of the inverse profiles of hardness and electrophilicity for the nH_2-trapped $B_{12}N_{12}$ clusters as monitored from Fig. 2 further indicates co-existence of the respective crests

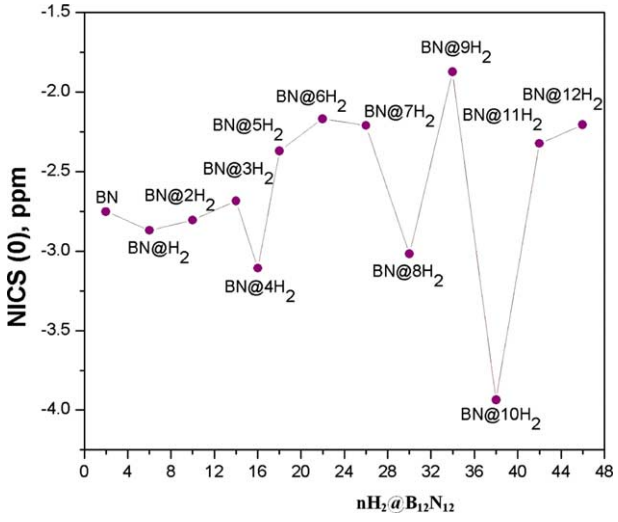

Fig. 3. Plot of cage aromaticity for $B_{12}N_{12}$ and different $nH_2@B_{12}N_{12}$ systems.

and troughs that unequivocally assigns a hard (higher η) species to have a low reactivity (lesser ω) and vice versa. An apparent odd–even oscillation in the ω profile of $nH_2@B_{12}N_{12}$ is discernible for certain n values. Fig. 2 also demonstrates a gradual fall off in the total energies of the nH_2-trapped $B_{12}N_{12}$ clusters upon increasing hydrogen storage, a trend quite familiar with cluster growth. The $E_{1E/H2}$ and E_{GE} plots for the plausible trapping reactions of molecular hydrogen with the $B_{12}N_{12}$ cage in spite of showing a quite favorable trend eventually lends stability to the nH_2-trapped $B_{12}N_{12}$ cage complex. A plot of the NICS(0) values at the cage centers of the various nH_2-trapped $B_{12}N_{12}$ clusters as a function of increasing cluster size delineated in Fig. 3 invokes the presence of aromaticity in all the aforesaid molecular motifs. But yet another peculiar behavior of the NICS(0) profiles analogous to that of the trends shown by the $E_{1E/H2}$ and E_{GE} demands further elucidation of facts to settle the stability criteria of the nH_2-trapped $B_{12}N_{12}$ clusters and to demand a facile usage of the $B_{12}N_{12}$ cage as a hydrogen storage medium in the future. Although the $E_{1E/H2}$ and E_{GE} profiles and the NICS(0) plot in Figs. 2 and 3, respectively, show an unexpected trend, a deeper insight into their dramatic behavior depicts some beautiful correlations that undeniably provokes to build a strong basis toward molecular stability. The E_{GE} values are supposed to dictate the stability criterion of a particular species upon comparing with its nearest neighbors. Based on this perspective, the E_{GE} profile illustrated in Fig. 2 depicts a trough and, hence, a local minimum at the positions assigned to $B_{12}N_{12}@3H_2$, $B_{12}N_{12}@6H_2$, and $B_{12}N_{12}@9H_2$. These moieties are thus less stable in comparison to their nearest neighbors. The η profile approximately shows a distinct lowering in these regions while the corresponding trends of ω creates

Citation: Nano Reviews 2011, **2**: 5767 - DOI: 10.3402/nano.v2i0.5767

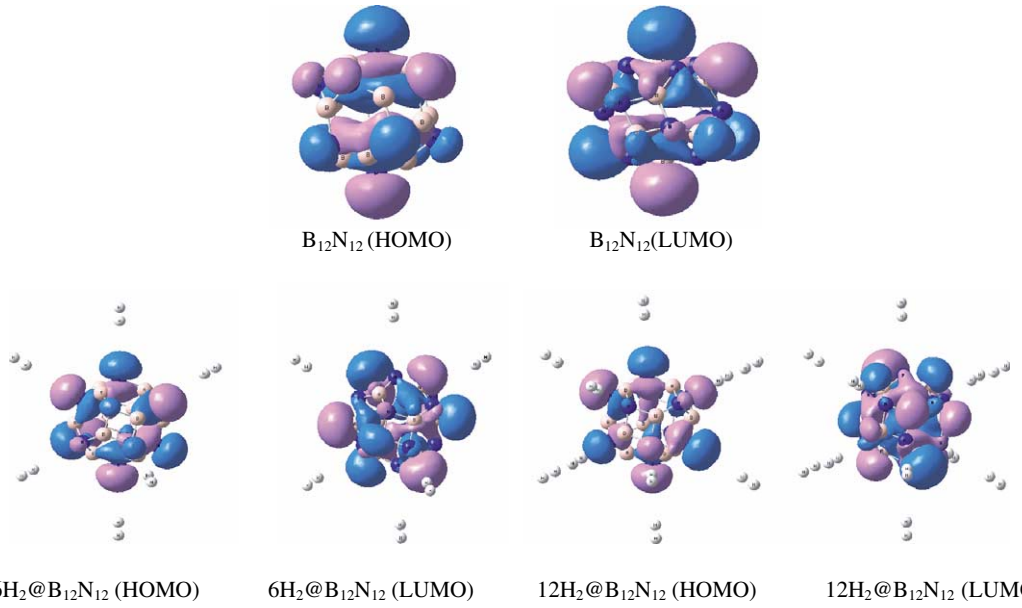

Fig. 5. Important frontier molecular orbital (HOMO and LUMO) pictures of $B_{12}N_{12}$ and some representative $nH_2@B_{12}N_{12}$ systems.

a hump in the same. Such a local instability criterion of these hydrogen bound $B_{12}N_{12}$ clusters is well corroborated from the NICS(0) profile in Fig. 3, which shows distinct peaks in these points occupied by $B_{12}N_{12}@3H_2$, $B_{12}N_{12}@6H_2$, and $B_{12}N_{12}@9H_2$ clusters. The visible local minima positions in the NICS(0) profile occupied by $B_{12}N_{12}@4H_2$, $B_{12}N_{12}@8H_2$, and $B_{12}N_{12}@10H_2$ clusters state that the former species are supposed to be stable owing to their highly aromatic nature. But the stability of the hydrogen bound $B_{12}N_{12}$ clusters as assigned in terms of an increasingly negative NICS(0) value cannot be successfully justified either from the corresponding E_{GE} curves or from that of the η and ω profiles. The aromaticity criterion, although proved to be widely popular and extremely relevant toward assigning stability to molecular clusters, might not be a sole decisive factor as already reported earlier (30). An IRC profile for the interaction of a single H_2 molecule with a BN system as depicted in Fig. 4 shows the entire reaction path visualizing the gradual approach of the molecular hydrogen toward the BN moiety that eventually passes through a transition state (with NIMAG = 1) to form a stable adduct species. The intrinsic reaction profile also portrays that the molecular hydrogen is essentially bound to the more electronegative N-center of the BN system. This fact is also clearly visible from the optimized structures of the corresponding nH_2-trapped $B_{12}N_{12}$ clusters in Fig. 1, which also depicts the involvement of the N-centers of the $B_{12}N_{12}$ cage toward trapping hydrogen. A considerable electronegativity difference between the N and B atoms might account for the preference of the N-centers over the B-centers as plausible attacking sites by molecular hydrogen. The important frontier molecular orbitals (FMOs) of the bare as well as nH_2-trapped $B_{12}N_{12}$ clusters show conspicuous electron delocalization in the cage moiety. Qualitative features of the FMOs do not change much on H_2-loading. Further work is in progress.

4. Conclusion

The possibility of using a $B_{12}N_{12}$ cage as a hydrogen storage material is analyzed in the light of conceptual DFT-based global reactivity descriptors, associated molecular electronic structure principles, and aromaticity. The variation of the different global reactivity descriptors as a function of gradual hydrogen loading onto the $B_{12}N_{12}$ cage complies with the deserving trends of the basic electronic structure principles that afford substantial stability upon cluster growth. A study of the different energy parameters governing a chemical reaction suggests that the gradual H_2-binding onto the $B_{12}N_{12}$ cage is spontaneous and energetically favorable. The stability of the nH_2-trapped $B_{12}N_{12}$ clusters is further substantiated from the presence of aromaticity in the $B_{12}N_{12}$ cage moiety. However, the aromaticity criterion is not supposed to be the sole determinant toward justifying molecular stability that, in fact, has been effectively considered through a subtle interplay between the fundamental conceptual DFT-based reactivity descriptors and the associated energy parameters that in turn affect chemical reactivity. Rates of adsorption and desorption of H_2 to and from BN also suggest a favorable kinetic behavior for this molecule to behave as a useful hydrogen storage medium.

Acknowledgements

We gratefully acknowledge the financial support from the Indo-EU (HYPOMAP) project. One of the authors (PKC) thanks DST, New Delhi for the J. C. Bose National Fellowship.

Conflict of interest and funding

There is no conflict of interest in the present study for any of the authors.

References

1. Department of Trade and Industry. The energy white paper: our energy future-creating a low carbon economy. Lincoln, UK: IEMA. Available from: http://www.iema.net/readingroom/articles?filter=167&aid=620; 2003 [cited 6 April 2011].
2. Schlapbach L, Züttel A. Hydrogen-storage materials for mobile applications. Nature (London) 2001; 414: 353–8.
3. Wang Q, Sun Q, Jena P, Kawazoe Y. Potential of AlN nanostructures as hydrogen storage materials. ACS Nano 2009; 3: 621–6.
4. Shevlina SA, Guo ZX. Transition-metal-doping-enhanced hydrogen storage in boron nitride systems. App Phys Lett 2006; 89: 153104–6.
5. Srinivasu K, Chandrakumar KRS, Ghosh SK. Quantum chemical studies on hydrogen adsorption in carbon-based model systems: role of charged surface and the electronic induction effect. Phys Chem Chem Phys 2008; 10: 5832–39, refs 2–12.
6. Peng Q, Chen G, Mizuseki H, Kawazoe Y. Hydrogen storage capacity of $C_{60}(OM)_{12}$ (M = Li and Na) clusters. J Chem Phys 2009; 131: 214505–12.
7. Wu G, Wang J, Zhang X, Zhu L. Hydrogen storage on metal-coated B80 buckyballs with density functional theory. J Phys Chem C 2009; 113: 7052–7.
8. Wagemans RWP, van Lenthe JH, de Jongh PE, van Dillen AJ, de Jong KP. Hydrogen storage in magnesium clusters: quantum chemical study. J Am Chem Soc 2005; 127: 16675–80.
9. McNelles P, Naumkin FY. A small molecule in metal cluster cages: $H_2@Mg_n$ (n = 8 to 10). Phys Chem Chem Phys 2009; 11: 2858–61.
10. Giri S, Chakraborty A, Chattaraj PK. Potential use of some metal clusters as hydrogen storage materials – a conceptual DFT approach. J Mol Model 2011; 17: 777–84
11. Sun Q, Wang Q, Jena P. Storage of molecular hydrogen in B-N cage: energetics and thermal stability. Nano Lett 2005; 5: 1273–7.
12. Wen SH, Deng WQ, Han KL. Endohedral BN metallofullerene $M@B_{36}N_{36}$ complex as promising hydrogen storage materials. J Phys Chem C 2008; 112: 12195–200.
13. Cui XY, Yang BS, Wu HS. Ab initio investigation of hydrogenation of $(BN)_{16}$: a comparison with that of $(BN)_{12}$. J Mol Struct (Theochem) 2010; 941: 144–9.
14. Parr RG, Yang W. Density functional theory of atoms and molecules. New York: Oxford University Press; 1989.
15. Geerlings P, De Proft F, Langenaeker W. Conceptual density functional theory. Chem Rev 2003; 103: 1793–874.
16. Chattaraj PK, Giri S. Electrophilicity index within a conceptual DFT framework. Ann Rep Prog Chem Sect C: Phys Chem 2009; 105: 13–39.
17. Chattaraj PK. Electronegativity and hardness: a density functional treatment. J Indian Chem Soc 1992; 69: 173.
18. Parr RG, Donnelly RA, Levy M, Palke WE. Electronegativity: the density functional viewpoint. J Chem Phys 1978; 68: 3801–7.
19. Parr RG, Pearson RG. Absolute hardness: companion parameter to absolute electronegativity. J Am Chem Soc 1983; 105: 7512–6.
20. Pearson RG. Chemical hardness: applications from molecules to solids. Weinheim: Wiley-VCH; 1997.
21. Parr RG, Szentpaly LV, Liu S. Electrophilicity index. J Am Chem Soc 1999; 121: 1922–4.
22. Chattaraj PK, Sarkar U, Roy DR. Electrophilicity index. Chem Rev 2006; 106: 2065–91.
23. Schleyer PVR, Maerker C, Dransfeld A, Jiao H, Hommes NJRVE. Nucleus-independent chemical shifts: a simple and efficient aromaticity probe. J Am Chem Soc 1996; 118: 6317–8.
24. Parr RG, Chattaraj PK. Principle of maximum hardness. J Am Chem Soc 1991; 113: 1854–5.
25. Ayers PW, Parr RG. Variational principles for describing chemical reactions: the Fukui function and chemical hardness revisited. J Am Chem Soc 2000; 122: 2010–8.
26. Chattaraj PK, Sengupta S. Popular electronic structure principles in a dynamical context. J Phys Chem 1996; 100: 16126–30.
27. Chamorro E, Chattaraj PK, Fuentealba P. Variation of the electrophilicity index along the reaction path. J Phys Chem A 2003; 107: 7068–72.
28. Frisch MJ, Trucks GW, Schlegel HB, Scuseria GE, Robb MA, Cheeseman JR, et al. Gaussian 03, Revision B.03, & GaussView. Pittsburgh, PA: Gaussian Inc; 2003.
29. Koopmans TA. On the classification of wavefunctions and eigen values of the individual electrons of an atom. Physica 1934; 1: 104–13.
30. Giri S, Abhijith Kumar RPS, Chakraborty A, Roy DR, Duley S, Parthasarathi R, et al. In: Chattaraj PK, ed. Aromaticity and metal clusters. Chapter 19, pp: 371–385, Boca Raton, FL: Taylor & Francis/CRC Press; 2010

***Pratim K. Chattaraj**
Department of Chemistry and Center for Theoretical Studies
Indian Institute of Technology Kharagpur
Kharagpur 721302
India
Email: pkc@chem.iitkgp.ernet.in

Citation: Nano Reviews 2011, **2**: 5767 - DOI: 10.3402/nano.v2i0.5767

Appendix

Table S1. Total energy (E_{Tot}, au), electronegativity (χ, eV), hardness (η, eV), electrophilicity (ω, eV) of different $nH_2@B_{12}N_{12}$ systems

Systems	E_{Tot} (au)	χ (eV)	η (eV)	ω (eV)
H_2	−1.14588	5.817	20.845	0.812
$B_{12}N_{12}$	−953.70670	5.174	12.233	1.094
$H_2@B_{12}N_{12}$	−954.85330	5.169	12.256	1.090
$2H_2@B_{12}N_{12}$	−956.00000	5.158	12.292	1.082
$3H_2@B_{12}N_{12}$	−957.14670	5.163	12.305	1.083
$4H_2@B_{12}N_{12}$	−958.29350	5.140	12.365	1.068
$5H_2@B_{12}N_{12}$	−959.44010	5.149	12.366	1.072
$6H_2@B_{12}N_{12}$	−960.58680	5.124	12.436	1.055
$7H_2@B_{12}N_{12}$	−961.73350	5.111	12.482	1.046
$8H_2@B_{12}N_{12}$	−962.88020	5.090	12.528	1.034
$9H_2@B_{12}N_{12}$	−964.02680	5.111	12.516	1.044
$10H_2@B_{12}N_{12}$	−965.17350	5.100	12.556	1.036
$11H_2@B_{12}N_{12}$	−966.32040	5.054	12.688	1.007
$12H_2@B_{12}N_{12}$	−967.46720	4.981	12.869	0.964

Table S2. The reaction electrophilicity ($\Delta\omega$, eV), interaction energy/molecule ($E_{IE/H2}$, eV), gain in energy (E_{GE}, eV) and chemisorption energy (E_{CE}, eV) computed for the binding of molecular hydrogen onto the $B_{12}N_{12}$ cage cluster

Systems	$\Delta\omega$(eV)	E_{IE/H_2}(eV)	E_{GE}(eV)	E_{CE}(eV)
$B_{12}N_{12}+H_2=H_2@B_{12}N_{12}$	−0.816	−0.499	0.502	0.499
$B_{12}N_{12}+2H_2=2H_2@B_{12}N_{12}$	−0.819	−0.508	0.515	0.508
$B_{12}N_{12}+3H_2=3H_2@B_{12}N_{12}$	−0.811	−0.510	0.515	0.510
$B_{12}N_{12}+4H_2=4H_2@B_{12}N_{12}$	−0.827	−0.513	0.521	0.513
$B_{12}N_{12}+5H_2=5H_2@B_{12}N_{12}$	−0.808	−0.510	0.496	0.510
$B_{12}N_{12}+6H_2=6H_2@B_{12}N_{12}$	−0.828	−0.506	0.483	0.506
$B_{12}N_{12}+7H_2=7H_2@B_{12}N_{12}$	−0.821	−0.510	0.533	0.510
$B_{12}N_{12}+8H_2=8H_2@B_{12}N_{12}$	−0.824	−0.509	0.502	0.509
$B_{12}N_{12}+9H_2=9H_2@B_{12}N_{12}$	−0.802	−0.505	0.477	0.505
$B_{12}N_{12}+10H_2=10H_2@B_{12}N_{12}$	−0.820	−0.504	0.502	0.504
$B_{12}N_{12}+11H_2=11H_2@B_{12}N_{12}$	−0.841	−0.514	0.615	0.514
$B_{12}N_{12}+12H_2=12H_2@B_{12}N_{12}$	−0.854	−0.519	0.577	0.519